# Radial Organization of Interstitial Exchange Pathway and Influence of Collagen in Synovium

F. M. Price,*‡ R. M. Mason,‡ and J. R. Levick*
*Department of Physiology, St. George's Hospital Medical School, and ‡Department of Biochemistry, Charing Cross and Westminster Medical School, London, England

ABSTRACT The synovial intercellular space is the path by which water, nutrients, cytokines, and macromolecules enter and leave the joint cavity. In this study two structural factors influencing synovial permeability were quantified by morphometry (Delesse's principle) of synovial electronmicrographs (rabbit knee), namely interstitial volume fraction $V_{v,I}$ and the fraction of the interstitium obstructed by collagen fibrils. Mean $V_{v,I}$ across the full thickness was 0.66 ± 0.03 SEM ($n$ = 11); but $V_{v,I}$ actually varied systematically with depth normal to the surface, increasing nonlinearly from 0.40 ± 0.04 ($n$ = 5 joints) near the free surface to 0.92 ± 0.02 near the subsynovial interface. Tending to offset this increase in transport space, however, the space "blocked" by collagen fibrils also increased nonlinearly with depth. Bundles of collagen fibrils occupied 13.6 ± 2.4% of interstitial volume close to the free surface but 49 ± 4.8% near the subsynovial surface (full-thickness average, 40.5 ± 3.5%), with fibrils accounting for 48.6–57.1% of the bundle space. Because of the two counteracting compositional gradients, the space available for fibril-excluded transport (hydraulic flow and macromolecular diffusion) was relatively constant >4 μm below the surface but constricted at the synovium-cavity interface. The space available to extracellular polymers was only 51–53% of tissue volume, raising their effective concentration and hence the lining's resistance to flow and ability to confine the synovial fluid.

## INTRODUCTION

The cavity of a diarthrodial joint is enclosed by a synovial lining (also called "intima" or "synovium"), which is a thin sheet of vascularized mesenchymal tissue 10–20 μm thick in the rabbit and 50–60 μm thick in humans. Synovium is responsible for the production and turnover of the lubricating fluid that occupies the joint cavity, and for the supply of nutrients to the avascular articular cartilage (Levick, 1984). This requires the transport of water, electrolytes, and nutrients from capillaries within the synovial lining into the joint cavity, and the drainage of fluid, metabolic end products, macromolecules, and cartilage degradation products from the joint cavity into the subsynovial lymphatic system (Davies, 1946; Yamashita and Ohkubo, 1993). Transport of these lipid-insoluble materials occurs chiefly by passive flow and/or diffusion through the intercellular spaces within the synovial lining. The lining comprises specialized fibroblast-derived "B cells" (synoviocytes) and tissue macrophages or "A cells" of bone marrow origin (Revell, 1989; Athanasou and Quinn, 1991; Wilkinson et al., 1992). The lining cells form a discontinuous layer separated by irregular intercellular gaps several microns wide (Knight and Levick, 1984; McDonald and Levick, 1988). The intercellular spaces abutting onto the joint cavity constitute the final common permeable pathway through which all hydrophilic exchange with intra-articular structures occurs. Conferring permeability is not the sole function of the intercellular pathways, however; they must also offer sufficient outflow resistance to retain a lubricant, the synovial fluid, within the joint cavity. The biophysical properties of the synovial intercellular pathway thus influence the volume and composition of synovial fluid.

The resistance of the synovial lining to transport depends partly on biochemical factors (i.e., the concentration of extracellular matrix biopolymers like hyaluronan, proteoglycans, glycoproteins, and microfibrils within the interstitial compartment) and partly on structural factors (Levick, 1994). The structural factors include the proportion of the tissue occupied by interstitium (the exchange pathway) and the proportion of interstitium occupied by collagen fibrils (fibrillar volume fraction), which present an obstacle to flow and macromolecular diffusion. These are the subject of the present investigation.

Fibril-forming collagens (types I, III, and V) are abundant, along with microfibril-forming type VI collagen (Ashhurst et al., 1991; Rittig et al., 1992). The fibrillar volume fraction influences the permeability of the pathway by several mechanisms (Levick, 1987): 1) Fibrils contribute to hydraulic drag. 2) Fibrils reduce the cross-sectional area available for transport. 3) They impose tortuosity on the transport pathway. 4) They exclude other biopolymers from a substantial fraction of the interstitial space. This last effect raises the effective concentration of matrix biopolymers in the pathway (i.e., the mass per unit volume of distribution), and this has a disproportionately large effect on transport resistance. Quantitative information on the collagen fibril space in synovium, as well as the interstitial space, is thus required for the achievement of a quantitative understanding of synovial permeability.

The present study was an essential prerequisite for the interpretation of glycosaminoglycan concentration in syno-

*Received for publication 24 February 1995 and in final form 12 July 1995.*
Address reprint requests to Prof. J. R. Levick, Department of Physiology, St. George's Hospital Medical School, London SW17 0RE England. Tel.: 181-725-5354; Fax: 181-725-2993.

0006-3495/95/10/1429/11 $2.00

vium, which was investigated in parallel with this work (preliminary report, Price et al., 1994). Glycosaminoglycan analysis results take the form of mass per unit tissue volume, whereas the physiologically relevant parameter (i.e., that governing transport resistance) is mass per unit extrafibrillar interstitial volume, as noted above. A primary purpose of this study was therefore to provide the data needed for the conversion of measured glycosaminoglycan concentration into extrafibrillar interstitial concentration, which can then be compared with measured hydraulic resistance and model simulations (Levick, 1991). Rabbit knee synovium was selected because its hydraulic permeability has been studied extensively.

Previous ultrastructural work has indicated that synovial cellularity is greater at the synovium-cavity interface than in a plane 5 $\mu$m below the surface (Levick and McDonald, 1989b). Collagen content, too, appeared to differ between these planes. It seemed likely, therefore, that the geometry and collagen content of the transport pathway might change systematically with depth. Another objective here was to establish the full depth profiles quantitatively so as to improve the precision of existing trans-synovial flow models.

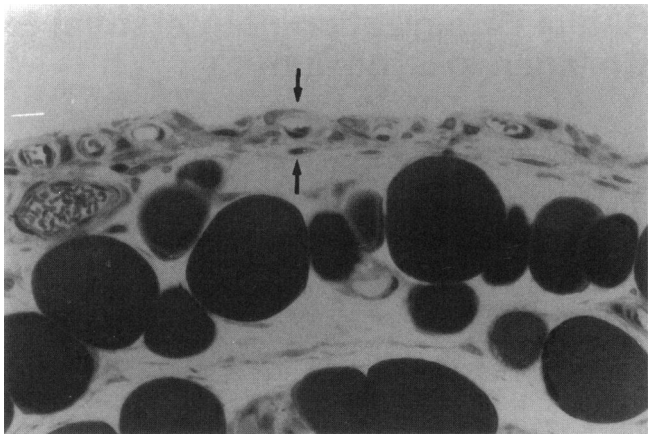

FIGURE 1 Photomicrograph of semithin section of synovial tissue excised en bloc from anterior rabbit knee, stained with toluidine blue. Cellular synovium with many capillaries is indicated by two arrows and abuts onto the joint cavity (*top*). Underlying subsynovium here contains adipocytes lying in loose areolar connective tissue. Plane of microdissection was approximately where the lower arrow is sited. Scale, ~15 $\mu$m between arrowheads.

## MATERIALS AND METHODS

### Harvesting of tissue

Synovium was microdissected from the knees of six freshly killed New Zealand white rabbits weighing 2–3 kg. Microdissection rather than bulk excision was used because the former is necessary for parallel analysis (to avoid contamination with subsynovium; parallel study) and it was clearly desirable to sample the tissue under the same conditions. The animals were killed by an intravenous overdose of sodium pentobarbitone (Euthatal, May and Baker, Ltd., Dagenham, U.K.) via the marginal ear vein. The knee was shaved and incisions were made parallel to and across the patellar ligament to provide access to the anterior compartment of the joint cavity. After the cavity was gently flushed with isotonic saline the animal was transferred into a humidity chamber. The chamber consisted of a polythene sheet draped over steel hoops mounted on the animal bench. Local humidity was maintained at >95% using an ultrasonic cool-vapor humidifier containing sterile distilled water, to prevent drying during dissection. Humidity was monitored by a dry-wet bulb thermohygrometer. The operator's arms could be pushed under the weighted free margins of the polythene side walls of the humidity chamber to provide manual access for dissection. A circular overhead aperture in the polythene tent gave access to the objective of a free-standing dissecting microscope (Zeiss OpMi-1, magnification ×16). With the animal in the chamber, the lateral and medial walls of the anterior compartment were retracted by weighted bulldog clips to expose suprapatellar areolar synovium, and the synovium was partially fixed in situ by superfusion with fixative for 1 min. This stiffened the synovial lining and facilitated its removal as a thin, uncollapsed sheet.

The synovial lining was microdissected from the underlying subsynovium using ultrafine ophthalmic microdissection instruments (John Weiss, Ltd., London). A small incision was made in the synovial surface with a 1.5-mm goniotomy knife, and the intima was separated from the loose underlying connective tissue (subsynovium) (see Fig. 1) by blunt dissection with a Troutman cyclodyalisis spatula or blunted Lang synechia knife. When the separation plane between subsynovium and the partially fixed, transparent synovial sheet had been established, a sliver of fine-textured filter paper (Whatman No. 50) soaked in fixative was slid under the partially freed synovial flap. This supported the specimen and kept it flat for later examination. The flap of synovium was then cut free with Roboz microdissection scissors and dropped into fixative. Synovium was dissected from the lateral side of one knee and the medial side of the opposite knee. Control studies showed that the in-built illuminating lamp of the dissecting microscope caused no detectable heating of the tissue at the working distance of approximately 20 cm.

### Tissue processing

The superfused fixative was 3% glutaraldehyde in 0.065 M sodium cacodylate buffer at pH 7.2, with 5% sucrose as osmotic buffer to minimize changes in cell volume during fixation as described by Bone and Denton (1971). The excised sample was placed in a vial of the same fixative for 18 h at 4°C. Subsequent processing took place at room temperature, with gentle agitation on a mixer at each step. After two 15-min rinses in the cacodylate buffer, tissue was post-fixed in 1% osmium tetroxide in 0.065 M sodium cacodylate buffer for 1½ h, followed by two further rinses. The synovial sheet, still supported on its subsynovial face by the filter paper, was then placed in a petri dish of buffer under a dissecting microscope and the filter paper was carefully removed.

For embedding, the sample was dehydrated by 30-min immersions in stepped concentrations of ethanol (30%, 70%, 90%, 100%, and 100%) followed by a pre-embedding fluid, propylene oxide. The sample was left overnight in a 50/50 mixture of propylene oxide and Spurr's epoxy resin on a slowly rotating mixer, followed by two soaks in fresh Spurr's resin for 3 h each with mixing. Finally, the flat sheet of tissue was orientated in the resin-filled embedding capsule to allow sectioning normal to the plane of the surface and was placed in an oven at 65°C for 24 h for polymerization.

### Sections

Gold-colored sections (estimated thickness, 60–90 nm) were cut normal to the plane of the surface with a glass knife on a Reichert-Jung ultramicrotome and were mounted on 200-mesh copper grids. Sections were stained with uranyl acetate (saturated solution in 70% ethanol) for 20 min, then washed and stained with 2% lead citrate for 20 min. Sections were examined in a Zeiss EM109 electron microscope at 80 kV. Two blocks were prepared per animal (one per joint), and three sections were photographed per block. An electron micrograph of the microdissected tissue is presented in Fig. 2.

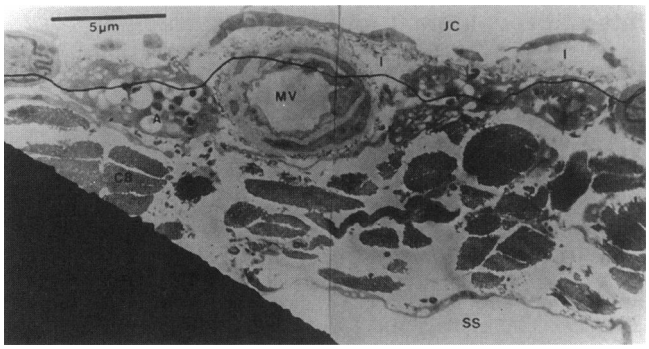


FIGURE 2 Composite electron micrograph of microdissected synovium. Line shows how a "slice" was demarcated for morphometric analysis of depth profile. JC, joint cavity. I, interstitium. A, macrophage or A cell. MV, microvessel. CB, collagen bundle. SS, subsynovium.

## Measurements

### *Interstitial volume fraction $V_{V,I}$*

This was estimated by a well-established point counting method based on Delesse's principle, viz., in a plane cut through a sample, the fraction of the total area occupied by a given material in that plane is equal to the fraction of the volume of the sample occupied by that material (Elias et al., 1971; Aherne and Dunnill, 1982). The fraction of the section area occupied by interstitium was estimated by replicate point counting. A square grid of points of spacing 5 mm, drawn on a transparent A4 acetate sheet, was laid over the photomicrograph of the section (average final linear magnification, ×4400, size A4). The number of points falling on interstitium was expressed as a fraction of the total points falling on the section to estimate the cross-sectional interstitial area fraction and hence the volume fraction. An estimate of the optimal number of points to be counted, $N$, was made, based on acceptable relative standard error (RSE)

$$\mathrm{RSE} = (1 - V_V)^{1/2}/N^{1/2}$$

where $V_V$ is the volume fraction (Aherne and Dunnill, 1982). For volume fractions of 0.6 and 0.3 (the range in the tissue) an $N$ value of 1000 gives a RSE of 2% and 3% respectively. For each electron micrograph at least 1000 points overlying synovium were therefore counted ($N$), and the number falling upon synovial cells or capillaries was noted ($n_c$). The interstitial volume fraction, $V_{V,I}$, was then estimated as $(N - n_c)/N$.

The above procedure was applied both to the full thickness of the synovium, to estimate the mean interstitial volume fraction, and to thin bands of synovium in a plane parallel to the surface to explore the variation in $V_{V,I}$ with depth. For the latter, lines were drawn on the electonmicrographs parallel to the surface at depth intervals of 2 μm as illustrated in Fig. 2. This defined a series of "slices" parallel to the surface, extending from cavity interface to subsynovial interface. The interstitial volume fraction in each slice was analyzed by point counting as above.

### *Interstitial area in planes parallel to surface ($A_{A,I}$)*

Measurement of the interstitial volume fraction in bands of finite thickness precludes analysis of the synovial surface itself. The relative area of cells and interstitium directly exposed to synovial fluid at the free surface was of interest because the pathway appeared to narrow considerably here. We therefore analyzed the fraction of the surface area occupied by interstitium in a plane parallel to the surface (i.e., en face) at 2-μm intervals, beginning at the synovium-cavity interface. The interstitial area fraction in a plane parallel to the surface ($A_{A,I}$) was estimated by the line intersection method (Aherne and Dunnill, 1982). A set of vertical lines 0.5 cm apart on an transparent (acetate) sheet was laid over the electron micrograph. The total number of intersections of lines with the plane of interest (e.g., synovial surface), $N_L$, and the number of intersections of the lines with the material of interest in that plane (interstitium), $n_L$, were counted. $A_{A,I}$ for that plane was calculated as $n_L/N_L$.

### *Collagen bundle volume fraction*

The fibrillar collagen of synovium is mostly organized into discrete collagen bundles (Fig. 2). The fraction of the interstitial space occupied by such bundles was estimated by counting the number of points falling within a bundle, $n_b$ (irrespective of whether the point fell on a fibril or on interfibrillar space within the bundle) and dividing this by the total number of interstitial points, $(N - n_c)$. Isolated fibrils not forming part of a bundle were neglected. The above procedure was applied to the full thickness of the synovium to estimate the mean collagen bundle volume fraction in interstitium and to each successive 2-μm-thick "slice" parallel to the surface (see above) to assess the variation with depth.

### *Fibril volume fraction within collagen bundle*

A collagen bundle comprises not only collagen fibrils but also space between the fibrils (Fig. 3). To estimate the fraction of the total extracellular space occupied by fibrils per se, the fraction of the bundle space occupied by fibrils was estimated. The latter also allows a theoretical estimate of the minimum hydraulic resistance to flow directly through a bundle, which seems to be novel (Appendix). Electron micrographs of bundle sections at high magnification (×60,000) were therefore analyzed by the point counting method. The number of points falling on collagen fibrils, $n_f$, was divided by the total number of points falling on the bundle, $n_b$, to determine the fibril volume fraction within a bundle.

### *Area fraction occupied by collagen in planes parallel to surface*

As noted above, the structure of the exchange pathway at the synovium-joint cavity interface is of particular interest. To assess the proportion of the surface and deeper planes occupied by collagen bundles, a line-counting procedure similar to that described above was used. The fraction of the interstitial surface area occupied by collagen bundles in a given plane was

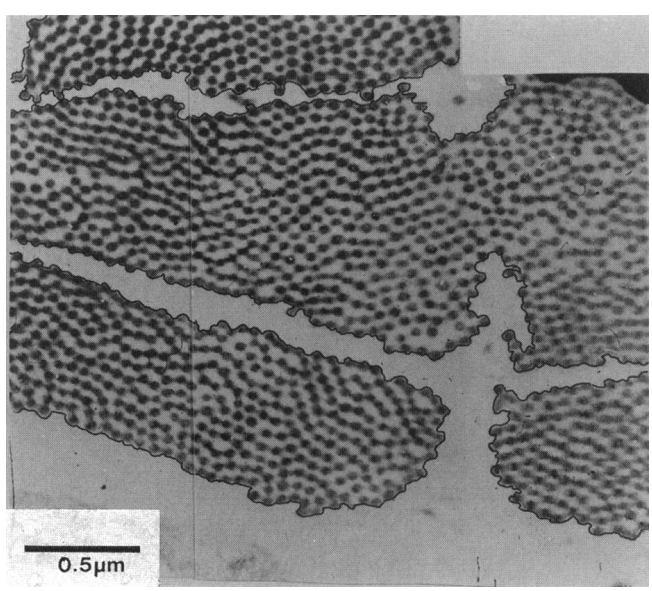


FIGURE 3 High-power electron micrograph of synovial collagen bundles in cross section. Each dark profile is a collagen fibril in cross section. Lines enclosing bundles show area analyzed.

estimated as the number of intersections of the superimposed lines with the collagen bundles in the chosen plane, $n_b$, divided by the total number of intersections of lines with interstitium in the plane of interest, $n_L$. $n_b/n_L$ was analyzed at 2-$\mu$m depth intervals commencing at the synovium-cavity interface.

### Statistics

Mean values are followed by standard errors of the mean throughout.

## RESULTS

### Synovial lining thickness

The arithmetic mean thickness of the synovial lining averaged 12.2 ± 0.9 $\mu$m for 31 sections from 11 joints of six rabbits. Thickness was uneven, both between joints and within a specimen, ranging from 6 to 23 $\mu$m (Fig. 4). When the thickness of a permeable membrane varies substantially, as here, the best measure of average thickness from the functional (i.e., permeability) viewpoint is the harmonic rather than arithmetic mean, i.e., the reciprocal of the mean of reciprocals of measured thickness (Weibel and Knight, 1964). This is because an uneven membrane comprises in effect a set of unequal permeabilities in parallel: each permeability is reciprocally related to thickness, and the parallel permeabilities summate. The harmonic mean thickness for microdissected synovium was 10.4 ± 0.7 $\mu$m, which is similar to that of suprapatellar areolar synovium fixed in situ at 5 cm $H_2O$ pressure and exised en bloc with a thick backing of subsynovium and muscle (harmonic mean, 12.0 ± 0.7 $\mu$m) (Levick and McDonald, 1989a).

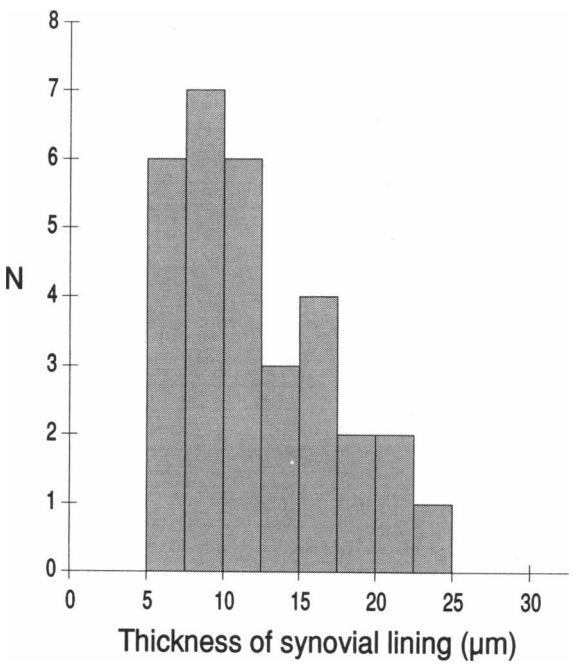


FIGURE 4 Histogram of thickness of microdissected synovial lining; $\Sigma N$ = 31 sections (11 joints, 6 rabbits). Arithmetic mean 11.5 ± 2.2 $\mu$m, range of 6–23 $\mu$m.

### Interstitial volume fraction and its gradient

Point counting over electron micrographs like that in Fig. 2 gave an average interstitial volume fraction $V_{V,I}$ of 0.66 ± 0.03 across the full thickness of the excised tissue (range, 0.52–0.79, $n$ = 31 sections, 11 joints). $V_{V,I}$ changed markedly, however, with depth (Fig. 5 *A*); it was smallest in the 2-$\mu$m-thick slice contiguous with the cavity, namely 0.398 ± 0.045, whereas by ~10 $\mu$m below the surface the interstitial volume fraction had more than doubled, to 0.921 ± 0.025. The increase in $V_{V,I}$ with depth was nonlinear, the rate of increase being greatest near the surface and much less at >6 $\mu$m. This depth analysis, being very laborious, was limited to five joints (one section per joint).

### Interstitial area fraction en face (plane parallel to surface, $A_{A,I}$)

As Fig. 5 *B* illustrates, 21.6 ± 4.9% of the synovial surface area at the synovium-cavity interface consisted of interstitial matrix in open contact with intra-articular fluid. The value

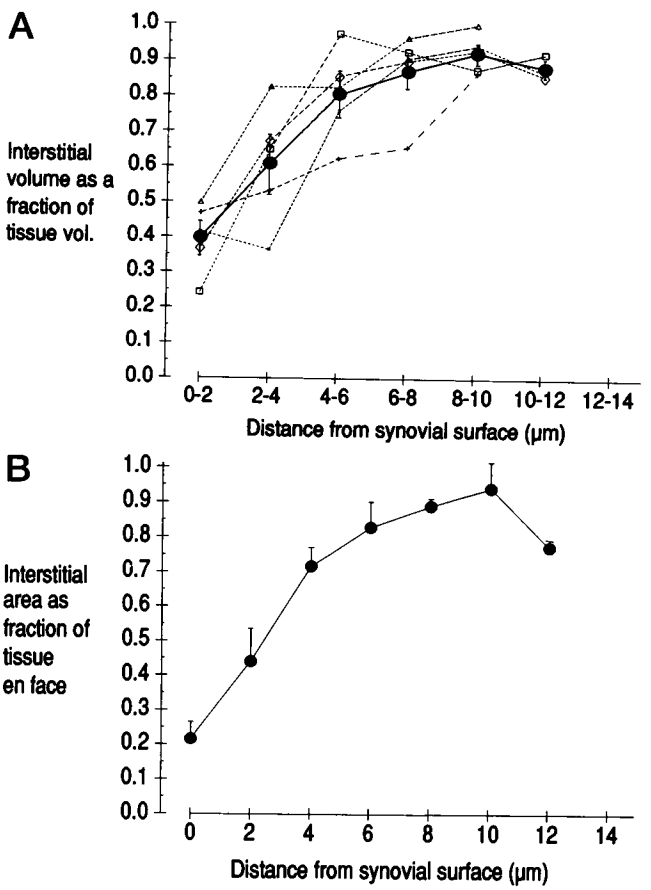


FIGURE 5 (*A*) Synovial interstitial volume in 2-$\mu$m-thick bands as a function of normal distance from synovium-cavity interface. Large circles are means with SEM bars. The individual profiles for five separate joints are shown as dashed lines. (*B*) Fractional area of synovium occupied by interstitium in planes parallel to surface at increasing depths. Means with SEM bars; $n$ = 5.

of $A_{A,I}$ at the surface (interface; 0.216), however, was smaller than at greater depths, because the cells extend many thin cytoplasmic processes over the synovium-cavity interface. The gradient of $A_{A,I}$ was especially steep close to the interface, with $A_{A,I}$ rising to 0.440 ± 0.095 at only 2 μm below the surface and 0.716 ± 0.054 at 4 μm. The area fraction then increased more gradually with depth, reaching 0.938 ± 0.022 at 10 μm from the surface, a value that reflects the paucity of cellular material at this depth.

## Volume fraction of collagen bundles within interstitium

The fraction of the interstitial volume occupied by collagen bundles across the full thickness of the lining averaged 0.41 ± 0.04 (11 joints, 31 sections). The range was relatively narrow in 10/11 joints, namely 0.32–0.56; the exception was a single joint with a bundle volume fraction of only 0.12. The distribution of the bundles showed a marked gradient normal to the free synovial surface (Fig. 6 *A*). There were very few collagen bundles in the 2-μm slice abutting onto the joint cavity (volume fraction 0.136 ± 0.024), in keeping with previous reports that type VI microfibrils and scattered type I/III/V fibrils are the characteristic features of interstitium near the interface (Levick and McDonald, 1989b, 1990; Ashhurst et al., 1991). Bundle density increased with distance from the cavity in a curvilinear fashion and approached a plateau of 0.451–0.489 of interstitial volume at distances greater than 4–6 μm from the surface.

## Area occupied by collagen bundles in plane parallel to surface

The paucity of organized collagen bundles near the surface was even clearer upon analyzing the surface area en face. Of the interstitial area exposed to joint fluid at the synovial surface, only 7.2 ± 4.4% was occupied by collagen bundles on average, and in 3/5 cases the value was zero. Thus although the interstitial pathway was narrowest at the surface (Fig. 5 *B*), it was also least obstructed by collagen bundles at the surface. The fraction of the interstitial area occupied by collagen bundles plateaued at values of 0.42–0.57 at distances of 6 μm or more from the surface.

## Fibril volume fraction within collagen bundle and within whole tissue

Application of the point counting method within the confines of synovial collagen bundles under high magnification indicated that collagen fibrils occupied 57.1 ± 3.7% of the space within a collagen bundle, the remainder being extrafibrillar space ($n$ = 4).

A potential source of overestimation of fibril volume fraction by the point counting method was noted, however, namely obliquity of some groups of fibrils relative to the

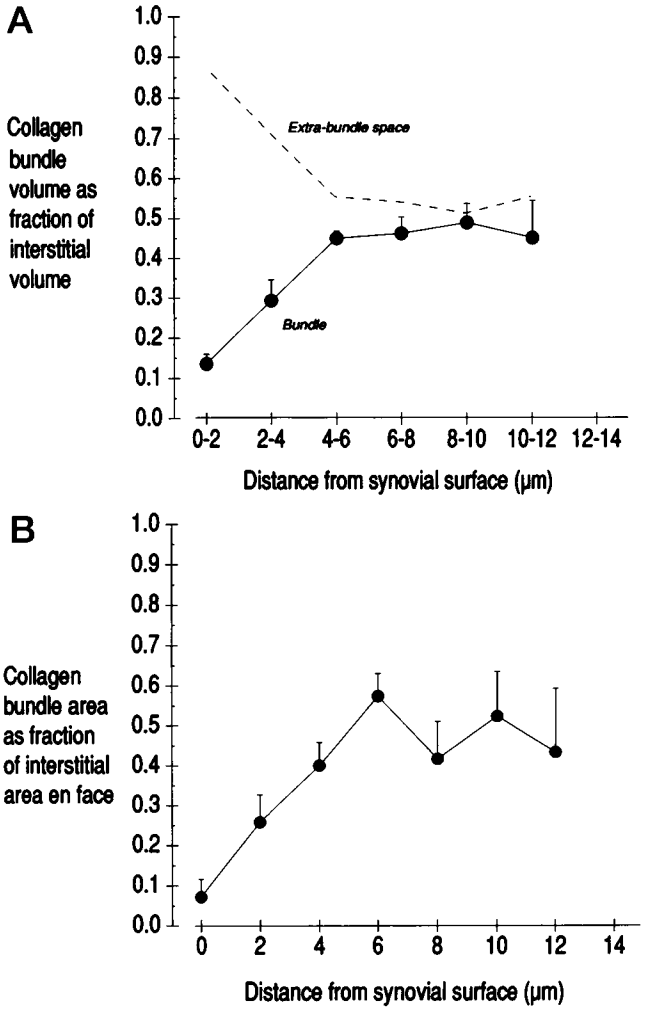


FIGURE 6 (*A*) Fraction of synovial interstitial volume occupied by collagen bundles, in 2-μm-thick bands at increasing distances from the synovium-cavity interface. Means with SEM bars. Dashed line is the fraction of the interstitium not occupied by bundles, $1 - [n_b/N - n_c]$. (*B*) Fraction of interstitial area occupied by collagen bundles in planes parallel to surface at increasing depths. Means with SEM bars. $n$ = 5.

plane of section (Fig. 3). Although the section angle is not a source of error in the morphometry of structures substantially bigger than the section thickness (e.g., the interstitial spaces, microns wide), the diameter of the collagen fibrils (55 nm) was of the same order of magnitude as section thickness (60–90 nm). For an oblique fibril running through a section viewed *en face*, there is an increased probability of a point falling (apparently) upon the densely stained fibril (which obscures over/underlying extrafibrillar space), leading to overestimation of fibril volume fraction. In an attempt to circumvent this problem, the number of fibril profiles was counted in a measured area of bundle section ($n_A$) and multiplied by the fibril cross-sectional area $\pi(d/2)^2$, the fibril being assumed to be cylindrical. Fibril diameter $d$ was taken to be the average of the minor axes of a set of fibril profiles. The chief uncertainty with this alternative procedure lay in measuring $\pi(d/2)^2$, because $d$ was small and any

error in measured $d$ was squared. In a large set of measurements on bulk-excised suprapatellar tissue from 15 rabbit knees, intrabundle fibril density was 172 ± 22 fibrils/$\mu m^2$ and fibril diameter 54.5 ± 3.0 nm, giving a calculated fibril volume fraction of 0.40 (McDonald 1988; Levick and McDonald 1989b); lower values (0.21–0.34) occur in adipose and posterior synovium. In the microdissected suprapatellar synovium here, intrabundle fibril density over an aggregate area of 3.0 $\mu m^2$ sectioned bundle was 168 $\mu m^{-2}$ (corresponding to an average center-to-center fibril spacing of 72 nm), fibril diameter was 55 nm, and calculated fibril volume fraction was 0.40. Fibril volume fraction by the point counting method over the same aggregate 3 $\mu m^2$ was 0.47 (0.466 and 0.475 by two independent observers). The point counting method may therefore have overestimated fibril volume fraction within the bundle by a factor of 0.47/0.40, or 1.175 times.

Combining the intrabundle fibril volume fraction with the fraction of interstitium occupied by collagen bundles (0.405), it was found that collagen fibrils occupied 19.7–23.1% of the total interstitial volume, neglecting scattered fibrils outside bundles (Table 1). Because interstitium formed 66.0% of the tissue volume on average, collagen fibrils occupied 13.0–15.3% of the synovial lining by volume (Table 1).

## Profile of free (noncollagen) pathway available for convective and diffusive transport

Collagen is an obstacle in the interstitial pathway. The proportion of the interstitial pathway not obstructed by collagen bundles was greatest near the surface (dashed line, Fig. 6), but, tending to offset this, the interstitial pathway was least extensive near the synovial surface (Fig. 5). We next assess the extent to which these opposing effects on transport space cancel out. Because the degree to which collagen impedes transport depends on the transport mode (i.e., whether hydraulic flow, diffusion of large solutes excluded from fibrils, or diffusion of small solutes able to permeate intrafibrillar water) (Maroudas, 1990; Maroudas et al., 1992), the above question was addressed separately for each transport process.

**TABLE 1 Collagen fibril parameters in synovium**

| | Parameter | Value |
|---|---|---|
| a | Interstitial volume as % tissue volume | 66 ± 3% |
| b | Collagen bundle volume as % interstitial volume | 40.5 ± 3.5% |
| c | Collagen fibril volume as % bundle volume | 48.6 –57.1%* |
| d | Collagen fibril volume as % interstitial volume (b × c) | 19.7 –23.1% |
| e | Collagen fibril volume as % tissue volume (a × b × c) | 13.0 –15.3% |
| f | Collagen molecule volume (partial specific volume) | 0.75 $ml \cdot g^{-1}$ |
| g | Collagen molecular mass per unit tissue volume‡ | $77.5 \times 10^{-3}$ $g \cdot ml^{-1}$ |
| h | Collagen molecular volume as % tissue volume ($f \times g$) | 5.8% |
| i | Fibril volume per g molecular collagen ($e$/100 $g$) | 1.68 –1.97 $ml \cdot g^{-1}$ |
| j | Fibril water content per g molecular collagen ($i-f$) | 0.93 –1.22 $ml \cdot g^{-1}$ |
| k | Fibril water content as % fibril volume ($j/i$) | 55–62% |

Values are averages for full thickness of lining. Bracketed entry shows method of calculation.

*Point-counting result (57.1%) divided by estimated obliquity error factor 1.175; see Results.

‡Price et al. (1994), corrected for specific gravity of sample 1.07.

### *Morphometric estimate of pathway for bulk flow*

The resistance to flow through the interior of a collagen fibril (i.e., through the intrafibrillar water space) is very high because of the dense packing of collagen molecules. Intrafibrillar resistivity is estimated to be $\sim 2 \times 10^{13}$ $dyn \cdot s \cdot cm^{-4}$ (Maroudas et al., 1987), and the effective intrafibrillar hydraulic radius only ~0.6 nm, so the resistivity for flow through a fibril is several orders of magnitude higher than resistivity for flow around it through the extrafibrillar matrix (Levick, 1987). Each collagen fibril thus acts as an effectively solid obstacle to flow. It is also necessary to consider whether the entire collagen bundle might behave as an effectively solid obstacle to flow; in other words, can a significant proportion of interstitial flow pass through a collagen bundle (as opposed to around it) via the spaces separating adjacent collagen fibrils within the bundle? The tiny size of these spaces, on the order of 22–54 nm wide (Fig. 3), coupled with the inverse power functions relating channel width to hydraulic resistance, implies a high resistance to flow within a bundle. Calculations based on hydrodynamic theory for flow through assemblies of cylindrical rods confirm this intuitive view (see Appendix) and indicate that the hydraulic resistivity (resistance of a unit cube of material) of a collagen bundle is likely to exceed that of the alternative pathway around the bundle through extrabundle interstitium.

Treating the collagen bundle is an effectively impervious obstacle to flow, the profile of the minimal flow pathway was calculated as the local interstitial volume fraction $V_{v,I}$ in each "slice" of synovium (Fig. 5 *A*) times the fraction of interstitium not occupied by collagen bundles (dashed line in Fig. 6 *A*). An analogous calculation was also made for the area available for flow in each plane *en face*. The results are shown by the filled circles in Fig. 7, *A* (volume fraction of flow pathway) and *B* (area fraction of flow pathway *en face*). The two structural gradients, increasing interstitial volume fraction and decreasing bundle-free fraction with depth, largely offset each other over much of the synovial thickness, producing a remarkably uniform fractional volume (0.43–0.47) available for extrabundle interstitial flow from 2–4 μm depth onward. Near the surface (0–2 μm), however, the flow pathway is smaller (fractional volume, 0.35). The relatively small area of the flow pathway at the actual cavity-synovium interface (0.24) is illustrated in

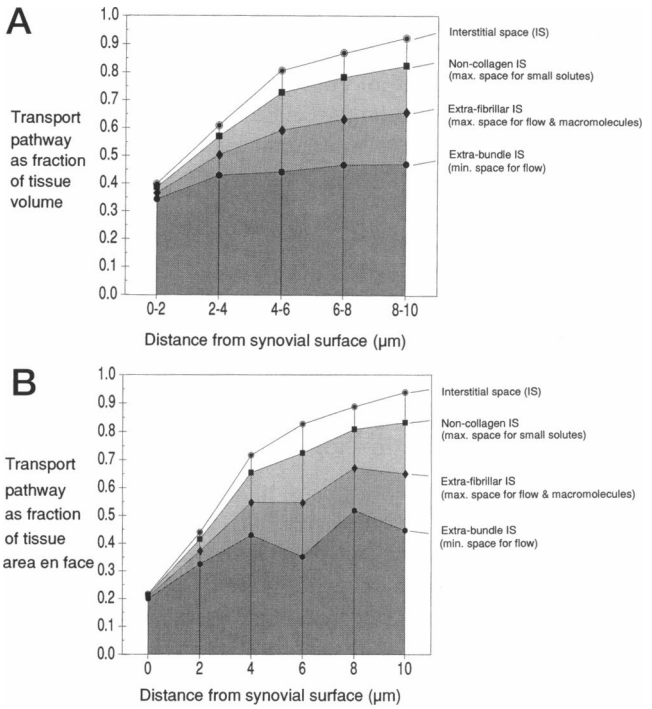


FIGURE 7 Change in geometric size of tranport pathway with distance across synovial lining, taking into account opposing effects of changing interstitial space (IS) fraction and collagen content with depth. See text for further explanation. (*A*) Volume fractions. (*B*) Area fractions. Mean results for five joints.

Fig. 7 *B*. Again, the *en face* area of the extrabundle flow pathway becomes more uniform at >4 μm from the surface.

The above calculation gives the minimum size of the synovial pathway conducting flow. If flow were to occur through the intrabundle extrafibrillar space as easily as around the bundle (unlikely, but not disproved absolutely; see Appendix), then the space available for hydraulic flow would be larger. Its upper limit is shown as filled diamonds in Fig. 7; these points represent interstitial volume minus fibril volume. The tendency toward uniformity in path volume (Fig. 7 *A*) and area (Fig. 7 *B*) at depths greater than 2–4 μm is again present, although the uniformity is not as good as for the extrabundle pathway. Again the path narrows near the surface.

### *Morphometric estimate of diffusion pathway for large solutes*

For macromolecules like albumin (Stokes-Einstein radius, 3.55 nm; molecular mass, 67,000 daltons), the fibril behaves as an impermeable rod (as with hydraulic flow) because the dense packing of the collagen molecules prevents macromolecules from permeating the intrafibrillar water space. The pore radius in the collagen molecular overlap regions is estimated to be only 0.6 nm, and even polyethylene glycols of molecular mass 6000 daltons are excluded (Maroudas et al., 1992). The interfibrillar spaces (width, 22–54 nm) separating the fibrils within a collagen bundle, however, are much wider than most solutes and have been shown to be accessible to small solutes in synovium (McDonald, 1988; Levick and McDonald, 1989b), although the rate of diffusion of macromolecules is likely to be restricted by steric and possibly electrostatic exclusion by interfibrillar proteoglycans. The maximum volume or area of the diffusion pathway for solutes of molecular mass > 6000 daltons was therefore the same as maximal flow pathway, namely $V_{V,I}$ × the fraction of interstitum not occupied by collagen fibrils. This is represented by filled diamonds in Fig. 7. The pathway increases in extent with depth, from 37% of the tissue volume at 0–2 μm to 66% at 8–10 μm. Similarly, the *en face* area available for diffusion increases with distance from the synovium-cavity interface. It is emphasized, however, that the geometical space only measures the *maximum* space available to solutes > 6000 daltons; steric exclusion by proteoglycans, etc., in the intrabundle, interfibrillar space, and the extrabundle interstitium, coupled possibly with electrostatic repulsion between fixed negative charges on glycosaminoglycans and negative charges on macromolecules, can be expected to reduce the actual available space to less than its geometrical value (Aukland and Reed, 1993).

### *Morphometric estimate of diffusion pathway for small solutes*

Very small solutes can diffuse through gaps beween individual collagen molecules and so permeate the intrafibrillar water space (Maroudas, 1990; Maroudas et al., 1992). For such solutes the fibril behaves as a porous rod composed of numerous thin cylinders (collagen molecules) with water occupying the intervening spaces (0.7–1.4 ml $H_2O$ per g collagen in nonsynovial tissues; Maroudas et al., 1992; review, Levick 1987). Consequently the space available for small solute diffusion is larger than for macromolecules or hydraulic flow and can be estimated as interstitial space minus collagen molecular volume (neglecting the small self-volume of other extracellular biopolymers). To estimate collagen molecular volume at each depth, using the measured fibril volumes, it is necessary to know fibril volume per gram of collagen. The latter is also a basic biophysical parameter and was assessed by combining the morphometric results with a published biochemical analysis for collagen as follows.

The average mass of molecular collagen in microdissected rabbit knee synovium, estimated via hydroxyproline analysis, was 77.5 mg/ml wet sample (Price et al., 1994). Because fibril volume fraction averaged 0.130–0.153 ml/ml synovium (Table 1, row e), the synovial collagen fibril had an average volume of 1.68–1.97 ml/g collagen (Table 1, row i). Subtracting the partial specific volume of molecular collagen (0.75 ml · $g^{-1}$), the noncollagen volume within a synovial fibril (presumably mainly water) was 0.93–1.22 ml/g collagen or 55–62% of the fibril volume. This was within the range found in other tissues (see above). The maximum space available for the diffusion of very small solutes is thus interstitial volume minus 38–45% of the

fibrillar volume. Across the full thickness of the lining this space is only 8.8% less than the interstitial volume; thus the space available for the transport of very small solutes is relatively little affected by collagen, unlike the space available for hydraulic flow. The depth profile of the diffusion space is plotted as filled squares in Fig. 7 for the 38% case (see above). This space expands continuously with depth, albeit nonlinearly, because the effect of the increase in interstitial volume fraction with depth outweighs the increase in collagen content with depth (cf. flow pathway).

## DISCUSSION

### Methodological considerations

The extent to which morphometric results are affected by tissue shrinkage during processing requires consideration. The osmotically buffered fixative used here produces relatively little cellular shrinkage (Maunsbach, 1966; Bone and Denton, 1971), so it is unlikely that the intercellular spaces were substantially enlarged by cellular shrinkage during fixation. In support, interstitial exposure at the surface of fixed synovium viewed by scanning electron microscopy is similar to that seen by light microscopy in normally hydrated synovium stained by silver nitrate (McDonald and Levick, 1988; Braun, 1884). The intercellular spaces are clearly not merely shrinkage "splits," because they are fully spanned by a glycosaminoglycan and collagen matrix (Highton et al., 1968; Okada et al., 1981; Levick and McDonald, 1990). The fact that the spaces are largest where the cell content is least (i.e., in the "deeper" slices) argues against the interstitial gradient being an artefact caused by cell shrinkage. The macroscopic linear shrinkage of rabbit synovium during processing, measured by a Vernier traveling microscope, is 4–8.5% (McDonald and Levick, 1988; Levick and McDonald, 1989b). Collagen fibril shrinkage, assessed by the shortening of the periodicity of the fibril banding pattern observed in electron micrographs, is a little greater, 7–11% (Levick and McDonald, 1990).

In light of the above, it is concluded that tissue processing may have had a minor but not substantial influence on the results for interstitial and collagen bundle volume fractions. The result for fibril volume per gram of molecular collagen (1.68–1.97 $ml \cdot g^{-1}$), however, is only a rough approximation for several methodological reasons. Fibril shrinkage during processing appears to be around 3% greater than overall tissue shrinkage (see above), leading to an underestimation of fibrillar volume fraction in vivo. Fibril volume fraction was also underestimated in that scattered fibrils outside bundles were not included. Biochemical analysis measures all collagens, including those that do not form fibrils, viz., type VI and type IV collagen, both of which are present (Pollock et al., 1990; Levick and McDonald, 1990); this will again lead to underestimation of fibril volume per gram of fibril-forming collagen. Errors acting in the opposite direction arise from the condensation of microscopic water droplets on the sample during microdissection in the humidity chamber, which reduces the apparent collagen mass per gram of tissue and so causes an overestimation of fibril volume per gram of collagen; and from the overestimation of the fibril volume/bundle volume ratio by point counting (see Results). The magnitude of several of these errors is uncertain at present.

### Comparisons with literature

To assess whether tissue manipulation during microdissection after the initial partial fixation might have altered tissue composition substantially, the results are compared below with results for rabbit suprapatellar areolar synovium excised en bloc or fixed in situ.

#### *Lining thickness*

The arithmetic mean thickness of microdissected lining here was 11.5 ± 2.2 μm, whereas that of areolar synovium excised en bloc was 15.6–17.6 μm (Knight and Levick, 1983). The harmonic mean, which is more relevant to transport resistance, was 10.2 ± 0.7 μm here, lying between the value of 12.0 ± 0.7 μm for synovium fixed in situ at 5 cm $H_2O$ intra-articular pressure and 9.1 ± 0.5 μm at 25 cm $H_2O$ (Levick and McDonald, 1989a).

#### *Interstitial exposure at surface*

The interstitial area fraction at the synovial surface here, 0.216, was within the range found in synovium excised en bloc (0.191–0.35; Knight and Levick, 1983; Levick and McDonald, 1989b). The high cellularity of the synovial surface here, 78%, closely matches a scanning electron microscopy study of tissue fixed in situ under normal intra-articular pressure, where cytoplasmic processes covered 74% of the synovial surface (McDonald and Levick, 1988).

#### *Interstitial area fraction at 5 μm depth*

The result here, 0.76 (mean of 4 μm and 6 μm values), was a little larger than at the same absolute depth en bloc (0.58–0.67). If depth is normalized to a percentage of thickness as the basis for comparison (the microdissected specimen being thinner), then at 22–26% of the full thickness (5 μm in the specimens en bloc, 2.5–3 μm here), the interstitial area fractions were 0.58–0.67 en bloc and slightly less (0.50–0.57) here.

#### *Interstitial volume fraction*

This has only previously been measured en bloc over a "slice" from 0 (surface) to 5 μm depth (0 to 22–26% of full thickness en bloc) and was 0.54–0.61. Here it was 0.546 over the band 0–5 μm or 0.48 over the 0–26% depth band (0–3 μm).

The above comparisons indicate that the harvesting procedure did not cause major alterations in interstitial volume and area fractions, but shape deformation by slight stretching cannot be excluded. It is known that the trans-synovial pathway is deformable, becoming thinner and broader when the synovial lining is stressed by high intra-articular pressures in pathological joint effusions (Levick and McDonald 1989a,b). Nevertheless, the interstitial volume fraction here is appropriate for the intended application, namely conversion of biochemical data obtained from tissue under identical sampling conditions into extrafibrillar concentrations.

## Significance of findings

The present results underpin the quantitative understanding of synovial permeability in several ways. 1) The full-thickness volume fraction value allows the conversion of measured glycosaminoglycan mass per unit tissue volume in a parallel study into the functionally meaningful mass per unit extrafibrillar interstitial volume. This is a vital step when attempting to explain the lining's known hydraulic resistance in terms of its biochemical composition (Levick and McDonald, 1995). 2) The information on the nonlinear relation between interstitial volume fraction and depth (normalized as a percentage of full thickness) will refine a quantitative, morphometry-based model of synovial permeability (Levick, 1991). 3) The collagen bundle results imply differences between the effective transport pathways for interstitial flow and for interstitial diffusion: this is an area of broad applicability, as well as being pertinent to models of trans-synovial macromolecular transport (Levick, 1994). These issues are considered more fully below.

### *Available space and thermodynamic concentration*

Interstitial permeability is dominated by the concentration of glycosaminoglycan, proteoglycans, and glycoproteins in the noncollagen interstitial space, with collagen also influencing permeability significantly (Levick, 1987). Measurements of biopolymer mass per unit tissue volume in a parallel study are of limited physiological usefulness in isolation, because the biopolymers are confined to the extracellular, extrafibrillar space (Maroudas, 1990), where their concentration is much higher; concentration in *available* space is the key parameter governing physiological function. Here, rabbit knee synovium was found to comprise 34% of cells and microvessels, and 13–15% collagen fibrils by volume (Table 1), leaving only 51–53% of the total tissue volume available to extracellular matrix biopolymers. These include chondroitin sulfate proteoglycans, heparan sulfate, hyaluronan, fibronectin, laminin, and probably keratan sulfate (Worrall et al., 1994; Pitsillides et al., 1994; Pollock et al., 1990; Price et al., 1994). Thus if glycosaminoglycan concentration is 1.7 mg/ml synovium by biochemical analysis (Price et al., 1994), its true, effective concentration in the transport pathway is almost double this, 3.2–3.3 mg/ml extrafibrillar space.

The finding that glycosaminoglycan available space is only half the tissue volume is particularly important in relation to the hydraulic resistance of the lining. Synovial hydraulic resistance is an important biophysical property because synovium has to function as a "skin" retaining synovial fluid within the joint cavity, as well as allowing diffusion of nutrients between the vascular compartment and joint cavity. Doubling the effective polymer concentration has a disproportionately large effect on hydraulic resistance because the relation between the two is nonlinear (see Appendix). The hydraulic resistance of a 1.7 $mg \cdot ml^{-1}$ glycosaminoglycan matrix is $0.25 \times 10^9$ $dyn \cdot s \cdot cm^{-4}$, whereas that of a 3.3 $mg \cdot ml^{-1}$ glycosaminoglycan matrix is $1.23 \times 10^9$ $dyn \cdot s \cdot cm^{-4}$. Thus, doubling the concentration raises the hydraulic resistance almost fivefold and supports the "skin" function of synovium.

### *Significance of structural gradient normal to surface*

The relatively high ratio of cell to interstitium at the interface with the joint cavity provides a large surface area for phagocytosis of intra-articular material by the macrophage-related A cells, and for hyaluronan/lubricin secretion into the cavity by the fibroblast-related B cells (synoviocytes). The increasing interstitial volume fraction and collagen fibril content with depth have functional implications both for tissue mechanics and for transport. Regarding mechanics, much of the overall tensile strength of synovium must reside in the deeper layers, because collagen bundle density reaches 49% there, in contrast to 13.6% near the surface. Regarding transport, the structural gradient affects the pressure and concentration profiles across the lining, as discussed next.

For *flow*, the volume fraction of the functional pathway was relatively uniform over much of the tissue's thickness, but close to the surface the narrowness of the intercellular gaps reduced the path area. From conservation of mass, the current velocity must therefore be higher in the surface zone than in the deeper zones for a given volume flow. This will require larger pressure gradients and/or a lower resistivity in the surface zone. This could be one reason why the composition of the superficial interstitial matrix differs, on ultrastructural evidence, from deeper zones; the superficial zone is characterized by a type VI microfibrillar network rather than dense, well-formed collagen bundles (Levick and McDonald, 1989b, 1990; Okada et al., 1990; Rittig et al., 1992).

The collagen distribution reported here is relevant to the modeling of trans-synovial flow. In the existing model (Levick, 1994), collagen was represented as randomly distributed fibrils occupying 20% of interstitial volume, which in itself is close to the average 24% found here. The effect of organization into collagen *bundles* that may constitute larger functional obstacles to flow was not considered in the existing model, however, and

indeed seems to have received little attention in the literature in general. The present study and Appendix indicate that collagen bundling should be incorporated in interstitial transport models wherever it occurs.

For *diffusion of small solutes*, the expansion of the permeable region with depth is much more marked than for bulk flow because of the ability of small solutes to permeate both interfibrillar and intrafibrillar water within the bundle. Given conservation of mass it follows that, for a solute that is undergoing steady-state diffusion, the concentration gradient must be steepest near the synovial surface and progressively less steep as the transport pathway widens in the deeper zones (to produce equal transport across the progressively expanding transport areas). The results thus imply the existence of nonlinear concentration gradients for small lipophobic solutes diffusing across synovium in the steady state.

In conclusion: the study provided quantitative ultrastructural information about the transport pathway into and out of joints. This information is necessary for the meaningful interpretation of biochemical measurements of extracellular materials (in hand) and should lead to refinement of models of physiological transport phenomena in synovium and other tissues with bundled collagen fibrils.

We thank Mr. R. Moss for training FMP in electron microscopy and the Wellcome Trust for project grant 031333/Z/90/A.

## APPENDIX: RESISTANCE TO FLOW WITHIN A COLLAGEN BUNDLE

Specific hydraulic resistivity, $R$, is the resistance to flow in a unit cube of material. For a material composed of long uncharged cylindrical fibers separated by fluid (as in a collagen bundle), resistivity can be estimated by Happel and Brenner's modification of the Carman-Kozeny equation (review, Levick 1987):

$$R = G_{HB}S^2/\epsilon^3 = G_{HB}/\epsilon r_h^2 \quad (1)$$

where $G_{HB}$ is a dimensionless Kozeny factor as modified by Happel and Brenner (1965) for matrices of cylindrical fibers, $S$ is fiber surface area per unit volume of matrix, $\epsilon$ is the void volume fraction, and $r_h$ is the mean hydraulic radius of the porosities of the matrix, equal to $\epsilon/S$. $G_{HB}$ is not a constant but is a function of $\epsilon$. Expanding the terms $\epsilon$ and $S$ for fibers of radius $r_f$ and solid volume fraction $\phi$ (equal to $1 - \epsilon$), the expression becomes

$$R = 4G_{HB}\phi^2/\{(1 - \phi)^3 r_f^2\} \quad (2)$$

Resistivity in a system of fibers can thus be calculated from fiber radius and fiber concentration. Happel showed that the value of $G_{HB}$ for fibers aligned at right angles to flow (the predominant orientation of synovial collagen bundles relative to trans-synovial flow) is approximated by

$$G_{HB,90°} = 2\epsilon^3/[(1 - \epsilon)[\ln\{1/1 - \epsilon\} - \{(1 - (1 - \epsilon)^2)/(1 + (1 - \epsilon)^2)\}]] \quad (3)$$

For void volume fractions 0.429 to 0.514, as determined for synovial collagen bundles here, $G_{HB,90°}$ is 5.31 to 5.39. Substituting $\phi = 0.571$ to 0.486 (present results) and $r_f = 27.5$ nm into Eq. 2, the internal resistivity of a collagen bundle to water at 35°C (viscosity 0.719 $\times$ $10^{-2}$ dyn · s · cm$^{-2}$) is calculated to be between 3.6 $\times$ $10^{10}$ and 8.3 $\times$ $10^{10}$ dyn s cm$^{-4}$. This may underestimate intrabundle resistivity in that proteoglycans span the intrabundle, interfibrillar spaces (Scott, 1988) and presumably introduce additional hydraulic drag.

A more rigorous theoretical treatment of flow at right angles to a regular array of uncharged cylinders was recently proposed by Tsay and Weinbaum (1991). For an unbounded array (i.e., negligible wall effects) their expression 42 shows that specific hydraulic conductivity $\kappa$ (cm$^2$; equal to $1/R$) is given by

$$\kappa = 0.0572r_f^2\left\{\left(\sqrt{\pi}/\sqrt{\phi}\right) - 2\right\}^{2.377} \quad (4)$$

This gives a predicted collagen bundle resistivity to water at 35°C of 7.1 $\times$ $10^{10}$ to 21 $\times$ $10^{10}$ dyn s cm$^{-4}$, somewhat higher than the Happel result. Expression 4 has not, to our knowledge, been compared with experimental data at volume fractions of interest here.

The resistivity of the collagen bundle must be compared with the resistivity of the surrounding interstitial matrix to assess its physiological significance. Synovial interstitial matrix contains at least 3.3 mg glycosaminoglycan/ml extrafibrillar space (biochemical analysis; Price et al., 1994) and perhaps as much as 13.9 mg long-chain biopolymer/ml inclusive of proteoglycans and glycoproteins (prediction of trans-synovial flow model; Levick, 1994). Application of the Kozeny-Happel-Brenner equation for randomly orientated fibers (a modification of Eq. 3) of concentration 3.3–13.9 mg · ml$^{-1}$, radius 0.56 nm, and partial specific volume 0.49 ml · g$^{-1}$ (characteristic values for glycosaminoglycan; Ogston et al., 1973; Comper and Zamparo, 1989) gives a predicted resistivity of 0.31 $\times$ $10^{10}$ to 2.7 $\times$ $10^{10}$ dyn s cm$^{-4}$ at 35°C. (The prediction of the Tsay-Weinbaum Eq. 4, which is limited to flow at right angles to fibers, is a little higher, 0.55 $\times$ $10^{10}$ to 3.4 $\times$ $10^{10}$ dyn s cm$^{-4}$.) By way of a yardstick it may be noted that the resistivity of articular cartilage, which has a very high proteoglycan and collagen concentration, is 2–3 orders of magnitude greater, viz., 126 $\times$ $10^{10}$ to 714 $\times$ $10^{10}$ dyn s cm$^{-4}$. An estimate of synovial extrafibrillar resistivity can also be made from the experimental results of Comper and Zamparo (1989, 1990) and Zamparo and Comper (1989). Their measurements of the specific hydraulic conductivity $\kappa$ (cm$^2$) of a proteoglycan matrix, namely chondroitin sulfate proteoglycan, can be summarized by the empirical formula

$$\kappa = 1.61 \times 10^{-18}\phi^{-2.354} \quad (5)$$

This predicts that the resistivity of a 3.3–13.9 mg · ml$^{-1}$ matrix is 0.12 $\times$ $10^{10}$ to 3.6 $\times$ $10^{10}$ dyn s cm$^{-4}$, a result of comparable magnitude to the above theoretical values.

Comparing the intrabundle resistivity with the extrabundle resistivity, we conclude that the minimal internal hydraulic resistivity of a synovial collagen bundle (3.6 $\times$ $10^{10}$ to 21 $\times$ $10^{10}$ dyn · s · cm$^{-4}$, even neglecting the hydraulic drag of intrabundle interfibrillar proteoglycans), exceeds that of the extrabundle matrix (range, 0.12 $\times$ $10^{10}$ to 3.6 $\times$ $10^{10}$ dyn s cm$^{-4}$). It is true that the highest estimate for extrabundle resistivity just equals the lowest estimate for intrabundle resistivity, but it must be borne in mind that true intrabundle resistivity is likely to be even higher than the estimate here because of the hydraulic drag of intrabundle interfibrillar proteoglycans. Given the difference in intra- versus extra-bundle resistivity, it is inferred that the whole collagen bundle acts as a functionally solid, log-like obstacle to trans-synovial flow, rather than as "brushwood" through which substantial flow occurs. Thus, most trans-synovial flow will divert around the collagen bundles, passing through the extrabundle interstitium. This must be taken into account in future models of interstitial flow.

## REFERENCES

Aherne, W. A., and M. S. Dunnill. 1982. Morphometry. London, Edward Arnold.

Ashhurst, D. E., Y. S. Bland, and J. R. Levick. 1991. An immunohistochemical study of the collagens of rabbit synovial interstitium. *J. Rheumatol.* 18:1669–1672.

Athanasou, N. A., and J. Quinn. 1991. Immunocytochemical analysis of human synovial lining cells; phenotypic relation to other marrow-derived cells. *Ann. Rheum. Dis.* 50:311–315.

Aukland, K., and R. K. Reed. 1993. Interstitial-lymphatic mechanisms in the control of extracellular fluid volume. *Physiol. Rev.* 73:1–78.

Bone, Q., and E. J. Denton. 1971. The osmotic effects of electron microscope fixatives. *J. Cell Biol.* 49:571–581.

Braun, H. 1884. Untersuchungen über den Bau der Synovialmembranen und Gelenkknorpel, sowie über die Resorption flüssiger, and fester Körper aus den Gelenkhölen. *Dtsch. Z. Chirurgie.* 39:35–86.

Comper, W. D., and O. Zamparo. 1989. Hydraulic conductivity of polymer matrices. *Biophys. Chem.* 34:127–135.

Comper, W. D., and O. Zamparo. 1990. Hydrodynamic properties of connective tissue polysaccharides. *Biochem. J.* 269:561–564.

Davies, D. V. 1946. The lymphatics of the synovial membrane. *J. Anat.* 80:21–23.

Elias H., A. Hennig, and D. E. Schwartz. 1971. Stereology: application to biomedical research. *Physiol. Rev.* 51:158–200.

Happel, J., and H. Brenner. 1965. Low Reynolds Number Hydrodynamics. Prentice-Hall, Englewood Cliffs, NJ. 392–404.

Highton T. C., D. B. Myers, and D. G. Rayns. 1968. The intercellular spaces of synovial tissue. *N Z Med. J.* 67:315–325.

Knight, A. D., and J. R. Levick. 1983. The density and distribution of capillaries around a synovial cavity. *Q. J. Exp. Physiol.* 68:629–644.

Knight, A. D., and J. R. Levick. 1984. Morphometry of the ultrastructure of the blood-joint barrier in the rabbit knee. *Q. J. Exp. Physiol.* 69: 271–288.

Levick, J. R. 1984. Blood flow and mass transport in synovial joints. *In* Handbook of Physiology, Section 2, The Cardiovascular System, Vol. IV, The Microcirculation. E. M. Renkin and C. C. Michel, editors. American Physiology Society, Bethesda. 917–947.

Levick, J. R. 1987. Flow through interstitium and other fibrous matrices. *Q. J. Exp. Physiol.* 72:409–438.

Levick, J. R. 1991. A two-dimensional morphometry-based model of interstitial and transcapillary flow in rabbit synovium. *Exp. Physiol.* 76:905–921.

Levick, J. R. 1994. An analysis of the interaction between extravascular plasma protein, interstitial flow and capillary filtration; application to synovium. *Microvasc. Res.* 47:90–125.

Levick, J. R., and J. N. McDonald. 1989a. Synovial capillary distribution in relation to altered pressure and permeability in knees of anaesthetized rabbits. *J. Physiol.* 419:477–492.

Levick, J. R., and J. N. McDonald. 1989b. Ultrastructure of transport pathways in stressed synovium of the knee in anaesthetized rabbits. *J. Physiol.* 419:493–508.

Levick, J. R., and J. N. McDonald. 1990. The microfibrillar meshwork of the synovial lining and associated broad-banded collagen—a clue to identity. *Ann. Rheum. Dis.* 49:31–36.

Levick, J. R., and J. N. McDonald. 1995. Fluid movement across synovium in healthy joints: rôle of synovial fluid macromolecules. *Ann. Rheum. Dis.* 54:417–423.

Maroudas, A. 1990. Different ways of expressing concentrations of cartilage constituents with special reference to the tissue's organization and functional properties. *In* Methods in Cartilage Research. A. Maroudas and K. Kuettner, editors. Academic Press, London. 211–219.

Maroudas, A., J. Mizrahi, E. Ben Haim, and I. Ziv. 1987. Swelling pressure in cartilage. Adv. Microcirc. 13:203–212.

Maroudas A., R. Schneiderman, and O. Popper. 1992. The role of water, proteoglycan and collagen in solute transport in cartilage. *In* Articular Cartilage and Osteoarthritis. K. Kuettner, R. Schleyerbach, J. G. Peyron, and V. C. Hascall, editors. Raven Press, New York. 355–371.

Maunsbach, A. B. 1966. The influence of different fixative and fixation methods on the ultrastructure of rat kidney proximal tubule cells. II. Effect of varying osmolarity, ionic strength, buffer system and fixative concentration of glutaraldehyde solutions. *J. Ultrastruct. Res.* 15: 283–293.

McDonald, J. N. 1988. Trans-synovial fluid dynamics. Ph.D. thesis. London University.

McDonald, J. N., and J. R. Levick. 1988. Morphology of surface synoviocytes in situ at normal and raised joint pressures, studied by scanning electron microscopy. *Ann. Rheum. Dis.* 47:232–240.

Ogston, A. G., B. N. Preston, and J. D. Wells. 1973. On the transport of compact particles through solutions of chain polymers. *Proc. R. Soc. A.* 333:297–316.

Okada Y., K. Naka, T. Minamoto, Y. Ueda, Y. Oda, I. Nakanishi, and R. Timpl. 1990. Localization of type VI collagen in the lining cell layer of normal and rheumatoid synovium. *Lab. Invest.* 63:647–656.

Okada Y., I. Nakanishi, and K. Kajikawa. 1981. Ultrastructure of the mouse synovial membrane; development and organisation fo the extracellular matrix. *Arthritis and Rheum.* 24:835–843.

Pitsillides, A. A., J. G. Worrall, L. S. Wilkinson, M. T. Bayliss, and J. C. W. Edwards. 1994. Hyalronan concentration in non-inflamed and rheumatoid synovium. *Br. J. Rheumatol.* 33:5–10.

Pollock, L. E., P. Lalor, and P. A. Revell. 1990. Type IV collagen and laminin in the synovial intimal layer: an immunohistochemical study. *Rheumatol. Int.* 9:227–280.

Price, F. M., J. R. Levick, and R. M. Mason. 1994. Quantification and localization of the glycosaminoglycans of rabbit synovium. Int. J. Exp. Pathol. 75:A27.

Revell, P. A. 1989. Synovial lining cells. *Rheumatol. Int.* 9:49–51.

Rittig, M., F. Tittor, E. Lütjen-Drecoll, J. Molenhauer, and J. Rauterberg. 1992. Immunohistochemical study of extracellular material in the aged human synovial membrane. *Mech. Ageing Dev.* 64:219–234.

Scott, J. E. 1988. Proteoglycan-fibrillar interactions. *Biochem. J.* 252: 313–323.

Tsay, R-Y., and S. Weinbaum. 1991. Viscous flow in a channel with periodic cross-bridging fibres: exact solutions and Brinkman approximation. *J. Fluid Mech.* 226:125–148.

Weibel, E., and B. W. Knight. 1964. A morphometric study on the thickness of the pulmonary air blood barrier. *J. Cell Biol.* 21:367–384.

Wilkinson, L. S., A. A. Pitsillides, J. G. Worrall, and J. C. W. Edwards. 1992. Light microscopic characteristics of the fibroblast-like synovial intimal cell (synoviocyte). *Arthritis Rheum.* 35:1179–1184.

Worrall, J. G., L. S. Wilkinson, and M. T. Bayliss. 1994. Zonal distribution of chondroitin-4-sulphate/dermatan sulphate and chondroitin-6-sulphate in normal and diseased human synovium. *Ann. Rheum. Dis.* 53:35–38.

Yamashita, S., and M. Ohkubo. 1993. Distribution and three-dimensional reconstruction of lymphatic vessels of the elbow joint capsule of rabbits. *Acta Anat. Nippon.* 68:513–521.

Zamparo, O., and W. D. Comper. 1989. Hydraulic conductivity of chondroitin sulfate proteoglycan. *Arch. Biochim. Biophys.* 274:259–269.